

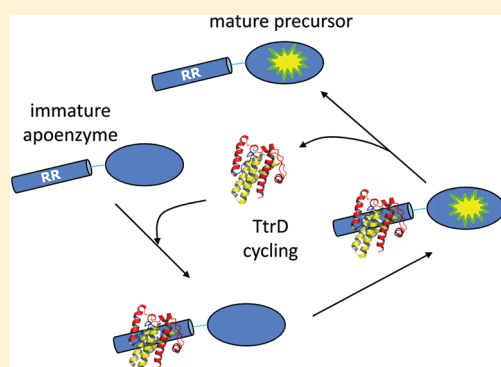
Conserved Signal Peptide Recognition Systems across the Prokaryotic Domains

Sarah J. Coulthurst, Alice Dawson, William N. Hunter, and Frank Sargent*

College of Life Sciences, University of Dundee, Dundee DD1 5EH, Scotland, United Kingdom

Supporting Information

ABSTRACT: The twin-arginine translocation (Tat) pathway is a protein targeting system found in bacteria, archaea, and chloroplasts. Proteins are directed to the Tat translocase by N-terminal signal peptides containing SRRxFLK “twin-arginine” amino acid motifs. The key feature of the Tat system is its ability to transport fully folded proteins across ionically sealed membranes. For this reason the Tat pathway has evolved for the assembly of extracytoplasmic redox enzymes that must bind cofactors, and so fold, prior to export. It is important that only cofactor-loaded, folded precursors are presented for export, and cellular processes have been unearthed that regulate signal peptide activity. One mechanism, termed “Tat proofreading”, involves specific signal peptide binding proteins or chaperones. The archetypal Tat proofreading chaperones belong to the TorD family, which are dedicated to the assembly of molybdenum-dependent redox enzymes in bacteria. Here, a gene cluster was identified in the archaeon *Archaeoglobus fulgidus* that is predicted to encode a putative molybdenum-dependent tetrathionate reductase. The gene cluster also encodes a TorD family chaperone (AF0160 or TtrD) and in this work TtrD is shown to bind specifically to the Tat signal peptide of the TtrA subunit of the tetrathionate reductase. In addition, the 3D crystal structure of TtrD is presented at 1.35 Å resolution and a nine-residue binding epitope for TtrD is identified within the TtrA signal peptide close to the twin-arginine targeting motif. This work suggests that archaea may employ a chaperone-dependent Tat proofreading system that is similar to that utilized by bacteria.



The twin-arginine translocation (Tat) pathway is a protein export system found in the cytoplasmic membranes of many prokaryotes (bacteria and archaea) and in the thylakoid membranes of plant chloroplasts.¹ The physiological function of the Tat system is the transmembrane translocation of fully folded proteins. Substrates are targeted to the Tat translocase by N-terminal signal peptides bearing an SRRxFLK “twin-arginine” amino acid motif.² Such Tat signal peptides have a tripartite structure comprising a polar n-region of variable sequence, followed by a hydrophobic h-region (15–25 amino acid residues) and a more polar c-region (often positively charged) that usually contains a protease cleavage site. The twin-arginine motif is positioned at the boundary between the n- and h-regions.²

The Tat translocase itself is membrane-embedded and contains a universally conserved TatC protein, which is involved in signal peptide recognition,³ a TatA-like protein that may form the protein-conducting channel,^{4–6} and, in some cases, a TatB component that forms a complex with TatC.³ The translocation event is driven by the transmembrane electrochemical gradient,⁷ and signal peptides are usually cleaved from substrates by membrane-bound signal peptidases.⁸

As a result of the ability of the Tat pathway to transport fully folded proteins, the vast majority of traffic following this route comprises enzymes that bind, and therefore fold around, cofactors in the cell cytoplasm prior to translocation. Clearly,

premature export of immature cofactor-containing enzymes must be avoided, and systems have been unearthed that coordinate the assembly and export events. Using an alkaline phosphatase reporter, Delisa et al.⁹ suggested that the Tat translocase itself may actively reject unfolded substrates. This was termed “Tat quality control”; however, the molecular basis of this phenomenon remains unresolved. In recent years, an alternative system designed to regulate transport on the Tat pathway by utilizing signal peptide-binding chaperones has been described. In this case, the signal peptides of immature Tat substrates are bound tightly by specific cytoplasmic proteins in a process that is hypothesized to suppress Tat transport until all other assembly processes are complete.¹⁰ Once cofactor insertion and protein folding has occurred, the signal peptide is released by the chaperone and is free to interact with the Tat translocase in the membrane. This system is termed “Tat proofreading”.¹⁰

The archetypal Tat proofreading chaperones belong to the TorD family.^{10,11} These are peptide-binding proteins dedicated to the assembly of molybdenum-dependent enzymes and include those required for biosynthesis of trimethylamine N-oxide

Received: December 14, 2011

Revised: January 29, 2012

Published: January 30, 2012



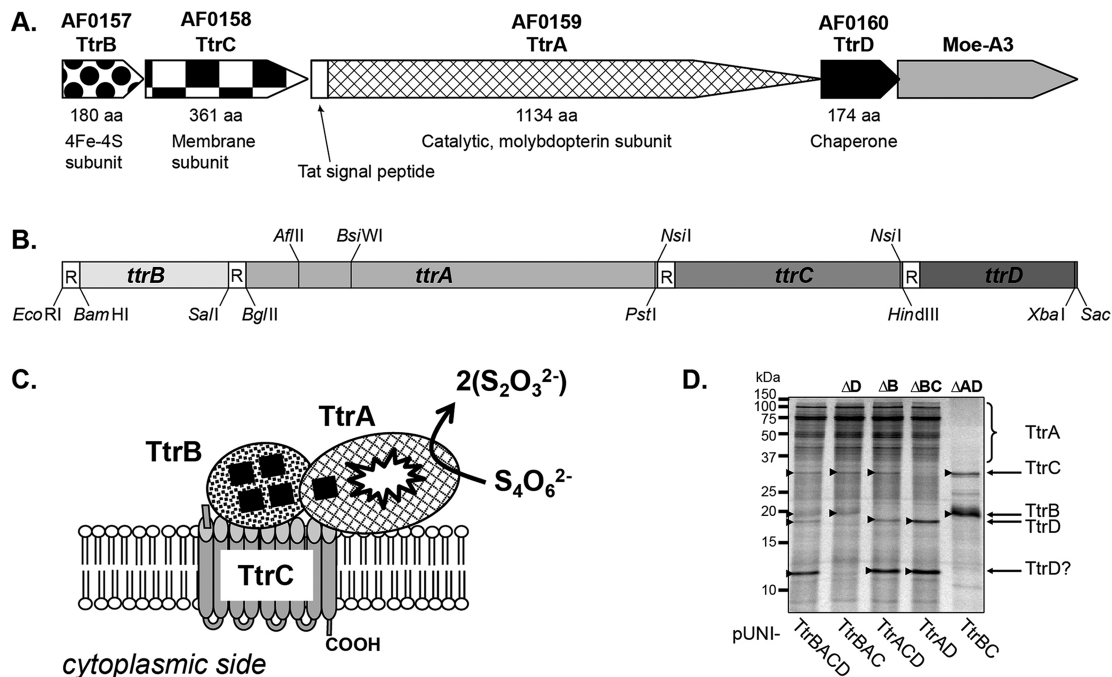


Figure 1. A putative tetrathionate reductase (*ttr*) operon in *Archaeoglobus fulgidus*. (A) Schematic representation of the AF0157–AF0161 operon from *A. fulgidus*. AF0157 (TtrB) is predicted to be an Fe–S protein, AF0158 (TtrC) is predicted to be an integral membrane protein with nine transmembrane domains, AF0159 (TtrA) is predicted to encode a Tat-dependent molybdenum- or tungsten-dependent reductase with most similarity to tetrathionate reductases from bacteria, TtrD is a member of the TorD family of signal peptide binding proteins, and Moe-A3 is a member of a family of proteins required for Mo or W incorporation into a pterin cofactor. (B) Schematic representation of a synthetic *ttrBACD* operon constructed in this study. Incorporated restriction sites are shown, and *E. coli*-biased ribosome binding sites are indicated by “R”. (C) A cartoon of how the *A. fulgidus* tetrathionate reductase may be assembled in the cell membrane. The black squares represent [4Fe–4S] clusters, and the white star represents the MGD cofactor. (D) ^{35}S -Met pulse-labeling of the Ttr proteins expressed from the synthetic operon under the control of the T7 promoter in pUNIPROM followed by SDS-PAGE and autoradiography. Derivatives of the pUNI-TtrBACD vector deleted for *ttrD* (ΔD), *ttrB* (ΔB), *ttrBC* (ΔBC), and *ttrAD* (ΔAD) are indicated.

(TMAO), dimethyl sulfoxide (DMSO), nitrate, and selenate reductases.^{12–15} Crystal structures of TorD family proteins show an α -helical fold arranged into two domains (N- and C-terminal) connected by a “hinge”. The proteins exist as monomers or domain-swapped homodimers where the N-domain of one protomer packs onto the C-domain of another.¹⁶ The hinge is often partially or completely unstructured and flexible, so many structures lack electron density for this region. This is a problem since the most highly conserved motif in TorD family proteins (EPxDH) is located within the hinge.¹⁶ The “DH” dipeptide is practically invariant and is essential for Tat proofreading activity,¹⁷ while biochemical and modeling studies have suggested these residues play a direct role in signal peptide recognition.^{15,18} TorD family proteins usually bind exclusively to one Tat signal peptide only, although one *Salmonella* chaperone has been shown to recognize three related Tat signal peptides.¹⁴ The molecular basis of peptide selectivity, or the peptide binding-and-release mechanism, is not fully understood, and the 3D structure of a signal peptide–chaperone complex is not available for any TorD family protein.

In an attempt to make new breakthroughs in understanding the Tat proofreading system in general, and the structure and function of TorD family chaperones in particular, the genetics of a number of microbes were studied. The hyperthermophilic archaeon *Archaeoglobus fulgidus* was found to carry the genes for several Tat-dependent reductases. One of those is a homologue of the *Salmonella enterica* tetrathionate reductase, an enzyme that has recently been implicated in the virulence of that human pathogen.¹⁹ Interestingly, a gene (Af0160) was

identified in the *A. fulgidus* *ttr* operon that would encode a TorD family protein which we named TtrD (Figure 1A). This observation suggests that assembly of these important enzymes may require a Tat proofreading chaperone.

In this work it is demonstrated that the TtrD protein binds directly to the twin-arginine signal peptide of the putative catalytic subunit of the *A. fulgidus* tetrathionate reductase. The binding epitope for TtrD on the signal peptide is identified as a short 11-residue stretch partly overlapping the conserved Tat motif. The high-resolution crystal structure of TtrD reveals a monomeric protein with a fold similar to some TorD family chaperones from bacteria. In this case, however, electron density corresponding to the hinge region is well-defined. This work suggests that archaea employ a Tat proofreading system during assembly of complex, cofactor-containing enzymes that is identical to that of bacteria.

MATERIALS AND METHODS

Bacterial Strains and Growth Conditions. Bacterial strains used in this study are listed in Table S1. *E. coli* strains were routinely cultured in LB media, at 37 °C and with appropriate antibiotic selection (Amp 100 $\mu\text{g}/\text{mL}$, Cm 25 $\mu\text{g}/\text{mL}$, and Kan 50 $\mu\text{g}/\text{mL}$). For SDS-resistance tests, SDS was added to LB agar plates at 2% (w/v) final concentration.

Plasmids and Molecular Biology. Plasmids used in this study are described in Table S1. All molecular biology was performed according to standard procedures. A synthetic *ttrBACD* operon was designed by back-translation of the amino acid sequences of the TtrBACD (AF0157-AF0160)

proteins from *A. fulgidus* DSM4303 (GenBank: AE000782.1) using the online Backtranslation tool (Entelechon, Germany). The sequence was also codon optimized for expression in *E. coli*. These sequences were then assembled into the synthetic operon *in silico*, with the concomitant introduction of ribosome binding sites and restriction sites for convenient downstream manipulation. Finally the complete 5.66 kbp sequence was synthesized and supplied in the cloning vector pGH (Biomatik) to yield pGH_SG1080110. The pUNI-TtrBACD plasmid was generated by the introduction of *ttrBACD* from the synthetic construct into pUNIPROM¹⁷ on a *Bam*H-I-XbaI restriction fragment. Subsequent derivatives were generated by removal of one or more *ttr* genes using their flanking restriction sites (Figure 1B). Other plasmids were generated by PCR amplification using oligonucleotide primers, the sequences and details of which are supplied in Table S2. For analysis of signal peptide function, the N-terminal 36 amino acids of TtrA ("ssTtrA") were expressed as an N-terminal genetic fusion to mature (signal peptide-lacking) AmiA in pUNIPROM (pUNI-ssTtrA_{AF}-AmiA), to mature BlaM in pSUPROM (pSU-ssTtrA_{AF}-Bla), or to GFP with a C-terminal SsrA tag in pBAD24 (pBAD-ssTtrA_{AF}-GFP-SsrA). For concomitant arabinose-inducible expression of TtrD, the synthetic *ttrD* gene was cloned into pBAD33. For TtrD protein purification, the synthetic *ttrD* gene was cloned into pETM-11 so as to allow IPTG-inducible expression of TtrD with an N-terminal 6-His tag followed by a TEV protease cleavage site (pETM-TtrD). For copurification analysis, pQE80 based plasmids were constructed expressing either His₆-GST or a ssTtrA-GST fusion protein, with or without the coexpression of untagged TtrD from the same plasmid (each protein cloned with a similar *E. coli* optimized ribosome binding site but both expressed from the vector TS promoter). Plasmids for bacterial two-hybrid analyses were constructed using the pUT18 and pT25 vectors.^{20,21} TtrD was fused to the C-terminus of T25 (pT25-TtrD) and ssTtrA fused to the N-terminus of T18 (pUT18-ssTtrA_{AF}). Single glutamine substitutions were incorporated into pUT18-ssTtrA_{AF} using the Quikchange procedure according to the manufacturer instructions (Agilent Technologies). *A. fulgidus* DSM4303 genomic DNA was kindly supplied by Clive S. Butler's group (University of Exeter, UK).

Expression and Production of Synthetic Gene Products. Expression of the *ttrBACD* genes from pUNI-plasmids can be controlled by the T7 promoter. *E. coli* strain K-38 was cotransformed with pGP1-2 (Kan^R), coding for the T7 RNA polymerase, and a pUNI-vector encoding the gene(s) of interest.²² Synthesis of gene products was induced by heat shock followed by radiolabeling with ³⁵S methionine.²² Proteins were separated by sodium dodecyl sulfate polyacrylamide gel electrophoresis (SDS-PAGE) before gels were fixed in 50% (v/v) methanol and 10% (v/v) acetic acid and analyzed by autoradiography.

Protein–Protein Interaction Analysis. BL21(DE3) and BL21(DE3) Δtat were transformed with pQE80-GST-ssTtrA or pQE80-GST-ssTtrA_{AF}. TtrD1 and expression of the GST fusion protein induced with 1 mM IPTG overnight at 19 °C. Cells were harvested and solubilized in B-Per (Pierce) containing protease inhibitors (Roche). GST fusion proteins were then isolated from the clarified bacterial extract by incubation (1 h, 4 °C) using glutathione Sepharose beads (GE Healthcare). The beads were washed three times with 20 mM HEPES pH 7.4, 1 M NaCl, 1 mM DTT, and 0.1% (v/v) Triton X-100. Finally, bound proteins were released from the beads by the addition of

sample buffer (1.6% (w/v) SDS, 50 mM Tris-HCl pH 6.8, 1.6 mM EDTA, 8% (v/v) glycerol, bromophenol blue) and visualized by SDS-PAGE and Coomassie staining. Copurifying proteins were identified by LC MS-MS (FingerPrints Proteomics Facility, University of Dundee).

Bacterial two-hybrid analyses were performed according to that described by Karimova and co-workers^{20,21} using the pUT18 and pT25 complementary pair of vectors. *E. coli* reporter strain BTH101 was transformed with pUT18-ssTtrA_{AF} (or derivative/control) and pT25-TtrD (or control), and the color of the resulting transformants scored on MacConkey media with 0.2% maltose (positive result being red). For quantitative measurement of the interaction, β -galactosidase assays were performed according to the method of Miller²³ on double-transformed BTH101 grown to exponential phase (or in the case of ssTtrA-RD and controls, to stationary phase) in LB and permeabilized with toluene. Assays were performed on at least three independent transformants.

Protein Purification. His₆-TtrD was overproduced from plasmid pETM-TtrD in *E. coli* BL21 (DE3) pLysS, and cells were harvested and broken in the presence of protease inhibitors (Calbiochem cocktail III). His₆-TtrD was isolated from the soluble fraction by immobilized metal affinity chromatography (IMAC) using a HiTrap (GE Healthcare) chelating column (20 mM Tris-HCl pH 7.5, 150 mM NaCl, 1 mM DTT, 25–500 mM imidazole). The His₆ tag was removed by TEV protease treatment (overnight digestion at room temperature in buffer: 50 mM Tris-HCl pH 7.5, 0.5 mM EDTA, 10% (v/v) glycerol, 2 mM DTT) and then noncleaved His-TtrD and TEV protease removed by reverse IMAC. Untagged TtrD was further purified using a Superdex 200 26/60 size-exclusion column (GE Healthcare) equilibrated with 50 mM Tris-HCl pH 7.5, 250 mM NaCl. The protein eluted as a single species with a mass consistent with that of a monomer. Selected fractions were pooled and concentrated to ~40 mg mL⁻¹ (2 mM) for crystallization trials. Sample purity was assessed by SDS-PAGE. The protein concentration was determined spectrophotometrically using a theoretical extinction coefficient of 13 410 M⁻¹ cm⁻¹.

Crystallization and Data Collection. Initial crystallization trials were performed using sitting drop vapor diffusion with standard sparse matrix screens and set up using a Rigaku Phoenix automated system. Equimolar amounts of a synthetic peptide (DFIKGLVAVGS) and 5 mM GMP-PNP were added to the protein prior to setting up crystallization experiments. Numerous conditions gave small crystals and optimization of selected conditions using hanging drop vapor diffusion then yielded diffraction quality crystals in three distinct forms from one (form I) previously deposited in the PDB (2idg). Crystal form II was obtained with 0.2 M potassium formate, 20% (w/v) PEG 3350 as the reservoir solution; form III with 0.1 M CHES pH 9.5, 20% (w/v) PEG 8K and form IV 4.3 M NaCl, 0.1 M HEPES pH 7.5. In each case crystals were obtained from drops containing 1 μ L of protein and 1 μ L of reservoir, at room temperature. Crystal forms II and III were obtained after the protein–peptide mix had been incubated on ice; crystal form IV was obtained when the mixture was heated to 70 °C. This resulted in some precipitation of the sample that had to be removed by centrifugation prior to crystallization. Crystals were flash cooled in liquid nitrogen, mounted on a goniostat, and maintained at -173 °C in a flow of cold nitrogen, and diffraction properties were characterized with a Rigaku Micromax 007 rotating anode R-AXIS IV⁺ image plate system. For crystal

forms II and IV, data were collected at the European Synchrotron Radiation Facility (Grenoble, France) on beamline ID29. The diffraction data for form III were collected in-house; however, due to a hardware fault, they are only 90% complete. Data were integrated using XDS (forms III and IV²⁴) and iMosflm (form II²⁵) and scaled with SCALA.²⁶ Crystallographic statistics are presented in Table S3. Coordinates for the three new crystal forms have been deposited in the PDB under accession codes 2xol, 2yjm, and 2y6y.

Structure Solution and Refinement. Each structure was solved by molecular replacement using PHASER.²⁷ For crystal form II, a model was generated from PDB entry 2idg (referred to as crystal form I). The structures of the other forms were solved using the refined monomer from form II. Rounds of model adjustment using Coot²⁸ interspersed with refinement calculations with Refmac5²⁹ were used to complete the protein model; the addition and refinement of water molecules and components of the crystallization mixture (1,2-ethanediol, N-cyclohexyl-2-aminoethanesulfonate, or Cl⁻) then completed the refinement. Translation/libration/screw (TLS) refinement using three domains (analysis was completed using the TLS server³⁰) was performed for crystal form IV and two domains for form III. Anisotropic thermal parameters were refined for form II. Despite the inclusion of a peptide in crystallization experiments, the electron density maps did not reveal any evidence for ordered binding.

RESULTS

A Synthetic Operon Encoding a Putative Tat-Dependent Tetrathionate Reductase. The genome of hyperthermophilic archaeon *A. fulgidus* encodes a putative tetrathionate reductase (Figure 1A). The genes in question are Af0157–Af0159, but for ease of understanding here, and in agreement with the *Salmonella* nomenclature,³¹ these have been renamed *ttrBCA* here (Figure 1A). *A. fulgidus* TtrA (1134 residues) is predicted to bear a twin-arginine signal peptide at its N-terminus and shares 30% overall sequence identity with the *Salmonella* TtrA protein (1020 residues). TtrA is therefore the putative catalytic subunit containing an N-terminal [4Fe–4S] cluster and a cysteine ligand (C297) to the metal component of a pterin cofactor. The *Salmonella* TtrA is known to utilize molybdopterin guanine dinucleotide (MGD) at its active site in order to catalyze the reductive cleavage of tetrathionate ($\text{S}_3\text{OS}-\text{S}-\text{S}-\text{SO}_3^-$ or $\text{S}_4\text{O}_6^{2-}$) to thiosulfate ($\text{S}-\text{SO}_3^-$ or $\text{S}_2\text{O}_3^{2-}$) and so confers the ability to use this unusual sulfur compound as a terminal electron acceptor during respiration.³¹ *A. fulgidus* TtrB is predicted to bind four [4Fe–4S] clusters and is most likely the electron-transfer partner of TtrA but bears no signal peptide of its own, and TtrC is predicted to be a membrane anchor/quinol dehydrogenase subunit containing nine transmembrane domains (Figure 1C). The overall architecture of this enzyme is therefore predicted to be a Tat-targeted heterodimer anchored to the extracytoplasmic side of the membrane by the TtrC subunit (Figure 4C).

A key feature of the *A. fulgidus* *ttr* operon is the presence of a gene encoding a putative Tat proofreading chaperone, TtrD (Figure 1A). To begin to understand the role of TtrD in assembly of tetrathionate reductase, a synthetic strategy was applied. The *A. fulgidus* protein sequences (TtrA-D) were “back-translated” into DNA sequence incorporating engineered ribosome binding- and restriction enzyme recognition-sites and biased toward *E. coli* codon usage (Figure 1B). The completely synthetic DNA sequence was arranged as *ttrBACD* to allow

facile removal of each gene from the 3' end and so leave the catalytic dimer intact. The synthetic operon was cloned into the *E. coli* expression vector pUNIPROM,¹⁷ and derivatives devoid of *ttrAD*, *ttrB*, *ttrBC*, and *ttrD* alone were prepared. Synthesis of the synthetic gene products in *E. coli* was monitored by ³⁵S-methionine labeling *in vivo* (Figure 1D). The expression and synthesis of TtrB and TtrC could be identified, especially when the *ttrA* and *ttrD* genes were removed from the vector (Figure 1D). TtrD could also be readily identified, though it may be susceptible to proteolysis (Figure 1D). However, it is clear from this experiment that the synthetic TtrA subunit is very unstable when expressed in *E. coli* and becomes rapidly fragmented (Figure 1D).

The *A. fulgidus* TtrA Signal Peptide Has Transport Activity in *E. coli*. The putative twin-arginine signal peptide of *A. fulgidus* TtrA shares 33% overall sequence identity, and 50% overall sequence similarity, with the TtrA signal peptide from *Salmonella* (over 30 amino acids). Given the close evolutionary relationship between *Salmonella* and *E. coli*, the *A. fulgidus* TtrA signal peptide was tested for Tat transport activity in *E. coli* (Figure 2).

One of the most sensitive *in vivo* Tat-transport assays available involves the Tat-dependent targeting of the amidase AmiA to the bacterial periplasm.³² An *E. coli* strain lacking periplasmic Tat-dependent amidases (MCDSSAC) cannot grow in the presence of 2% (w/v) SDS (Figure 2A) as the protective barrier of the cell envelope is weakened.³² However, this phenotype can be complemented by providing a Tat-targeted amidase (e.g., AmiA) *in trans*. In this work the mature *E. coli* AmiA enzyme was genetically fused to the *A. fulgidus* TtrA N-terminus (residues 1–36). When this fusion was expressed in MCDSSAC, it was observed to restore the ability of the strain to grow in the presence of SDS (Figure 2A). This demonstrates that the N-terminal region of TtrA contains an active twin-arginine signal peptide that can direct AmiA to the *E. coli* periplasm.

This finding was corroborated with a second *in vivo* Tat-transport assay. *E. coli* is normally sensitive to the antibiotic ampicillin unless a periplasmic β -lactamase (Bla) is expressed. The Bla catalytic domain can be exported in a Tat-dependent manner.³³ In this case the *A. fulgidus* TtrA signal peptide was genetically fused to Bla and the ability of this fusion to confer resistance to ampicillin tested (Figure 2B). Production of the TtrA signal peptide-Bla fusion was indeed able to confer ampicillin resistance on *E. coli* (Figure 2B), and this phenotype was completely abolished in a Tat transport mutant (Figure 2B).

TtrD Interacts Directly with the TtrA Signal Peptide. TorD family chaperones are renowned for their ability to bind directly to twin-arginine signal peptides or inactive remnants of such peptides.^{10,34} To assess the ability of TtrD to bind to the TtrA signal peptide, small-scale copurification experiments were designed (Figure 3). The TtrA Tat signal peptide (residues 1–36) was genetically fused to the N-terminus of glutathione-S-transferase (GST) and expressed alone, or in the presence of TtrD, in *E. coli* (Figure 3). The GST was then isolated using glutathione beads and copurifying proteins identified following SDS-PAGE and mass spectrometry (Figure 3). It is clear from these experiments that TtrA-GST copurified with a single protein, which was unambiguously identified as *A. fulgidus* TtrD (Figure 3). No endogenous *E. coli* Tat proofreading chaperones, or any other *E. coli* proteins, were found to interact with TtrA-GST. Interestingly, the amount of copurifying TtrD was enhanced by coexpression of TtrA-GST in a Δtat mutant

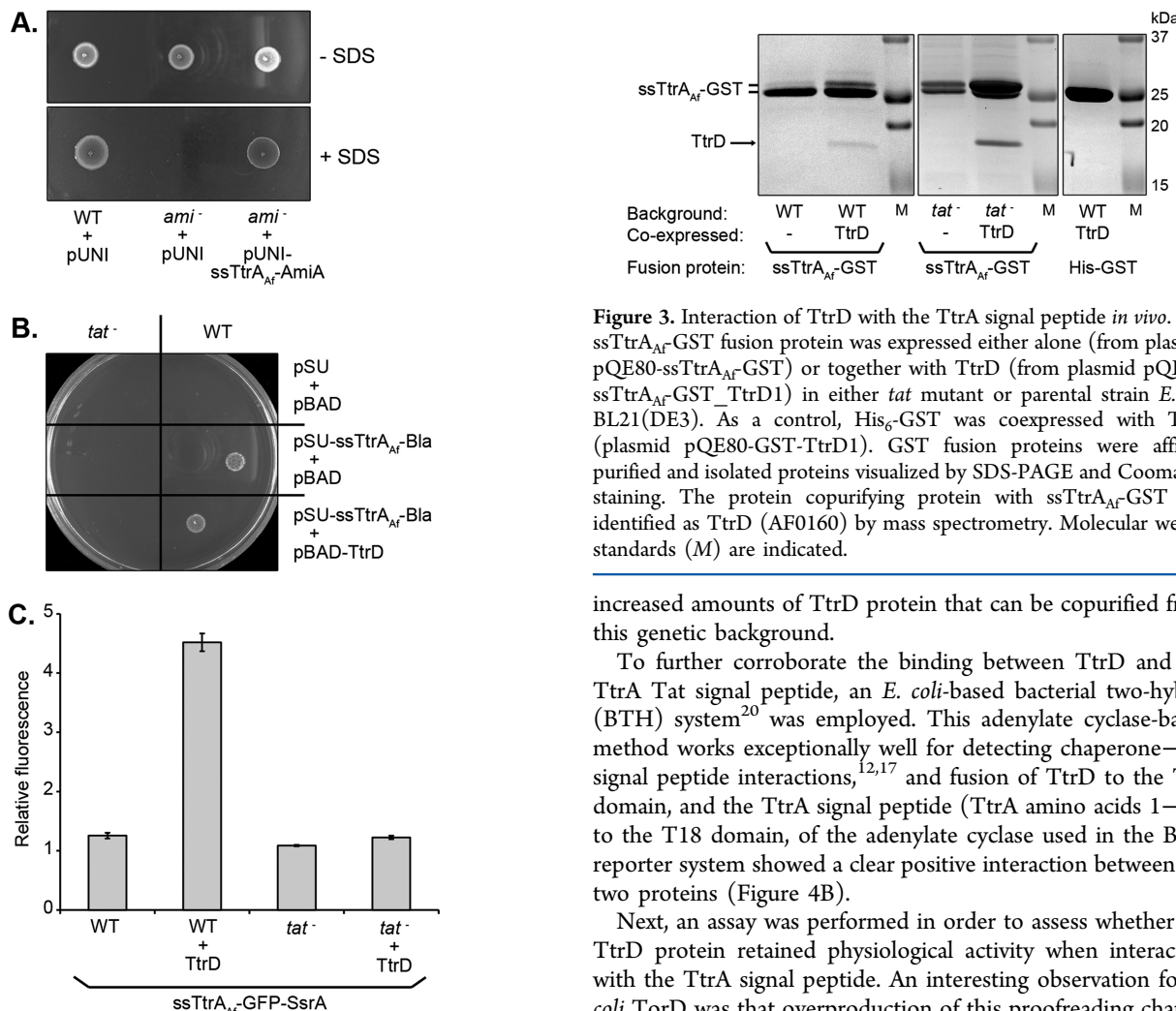


Figure 2. The N-terminus of TtrA contains an active twin-arginine signal peptide. (A) SDS-resistance (Tat-dependent amidase export) assay. Parental strain (WT) or *amiAC* mutant *E. coli* (strains MC4100 and MCDSSAC, respectively) carrying pUNIPROM (pUNI, vector control) or pUNI-ssTtrA_{Af}-AmiA (expressing an ssTtrA_{Af}-AmiA fusion protein) were grown aerobically on LB plates containing 2% (w/v) SDS where indicated. (B) Tat-dependent β-lactamase (Bla) transport assay. Parental strain (WT) or *tatABCD* mutant (*tat*⁻) *E. coli* (strains MC4100-A and DADE-A, respectively) were transformed with a plasmid encoding the *A. fulgidus* TtrA signal peptide fused to signalless β-lactamase (pSU-ssTtrA_{Af}-Bla) and a vector encoding TtrD (pBAD-TtrD). Control plasmids were pSUPROM (pSU) and pBAD33 (pBAD). Overnight cultures of each strain were diluted 10⁻⁴ and 10 μL spotted onto an LB plate supplemented with Kan (50 μg/mL), Cm (25 μg/mL), Amp (6 μg/mL), and L-arabinose (0.2% w/v). (C) TtrD enhances the transport activity of the TtrA signal peptide. *E. coli* strains MC4100-A (WT) and DADE-A (*tat*⁻) were each transformed with pBAD-ssTtrA_{Af}-GFP-SsrA (or vector control pBAD24) and pBAD-TtrD (or vector control pBAD33) and grown aerobically in LB containing Amp (100 μg/mL), Cm (25 μg/mL), and arabinose (0.2% w/v). GFP fluorescence was measured after 18 h. The fluorescence for each strain carrying pBAD-ssTtrA_{Af}-GFP-SsrA is expressed relative to the background fluorescence of the parent strain carrying the vector control plasmids. Bars show mean ± SEM.

background (Figure 3). Indeed, inspection of the SDS-PAGE gel suggests that the full-length TtrA signal peptide-GST fusion is less susceptible to proteolysis when expressed in the *E. coli* Δtat strain (Figure 3) and that this probably accounts for the

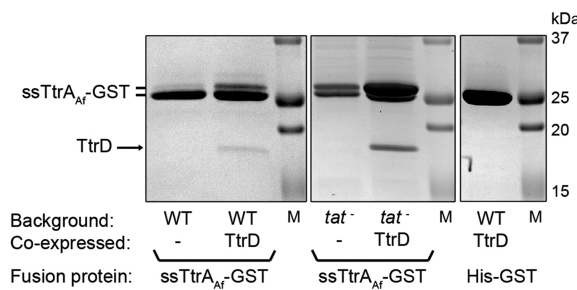


Figure 3. Interaction of TtrD with the TtrA signal peptide *in vivo*. The ssTtrA_{Af}-GST fusion protein was expressed either alone (from plasmid pQE80-ssTtrA_{Af}-GST) or together with TtrD (from plasmid pQE80-ssTtrA_{Af}-GST_TtrD1) in either *tat* mutant or parental strain *E. coli* BL21(DE3). As a control, His₆-GST was coexpressed with TtrD (plasmid pQE80-GST-TtrD1). GST fusion proteins were affinity purified and isolated proteins visualized by SDS-PAGE and Coomassie staining. The protein copurifying protein with ssTtrA_{Af}-GST was identified as TtrD (AF0160) by mass spectrometry. Molecular weight standards (M) are indicated.

increased amounts of TtrD protein that can be copurified from this genetic background.

To further corroborate the binding between TtrD and the TtrA Tat signal peptide, an *E. coli*-based bacterial two-hybrid (BTH) system²⁰ was employed. This adenylate cyclase-based method works exceptionally well for detecting chaperone–Tat signal peptide interactions,^{12,17} and fusion of TtrD to the T25 domain, and the TtrA signal peptide (TtrA amino acids 1–36) to the T18 domain, of the adenylate cyclase used in the BTH reporter system showed a clear positive interaction between the two proteins (Figure 4B).

Next, an assay was performed in order to assess whether the TtrD protein retained physiological activity when interacting with the TtrA signal peptide. An interesting observation for *E. coli* TorD was that overproduction of this proofreading chaperone could enhance the Tat-dependent export of a fusion between the TorA signal peptide and green fluorescent protein (GFP).³⁵ To reconstruct this assay for the *A. fulgidus* system under investigation here, a plasmid was constructed encoding a fusion between the TtrA signal peptide and GFP bearing an SsrA tag (Figure 2C). An SsrA tag is a short C-terminal sequence (...AANDENYALAA-COOH) that will target any protein for degradation by cytoplasmic proteases.³⁶ However, transport of an SsrA tag-containing protein to the periplasm protects it from degradation and in the case of Tat-dependent targeting of GFP-SsrA therefore leads to an increase in GFP fluorescence in a *tat*⁺ strain compared to a *tat* mutant.³⁶ In this work, production of the ssTtrA-GFP-SsrA fusion alone in Tat-active *E. coli* led to a very low level of fluorescence, pointing to a rate of export for this fusion protein that is too slow to escape proteolytic degradation (Figure 2C). However, coexpression of TtrD with the ssTtrA-GFP-SsrA fusion protein in the same strain lead to a clear increase in cellular GFP fluorescence (Figure 2C). This TtrD effect was not evident in a *tat*⁻ background (Figure 2C), which taken together suggests the functional interaction between the chaperone and the signal peptide can enhance the rate or efficiency of transport of GFP-SsrA on the Tat pathway.

Collectively, these experiments demonstrate that TtrD is a signal peptide-binding protein and that at least one of its binding partners in *A. fulgidus* is the Tat-targeted reductase with which it is coexpressed.

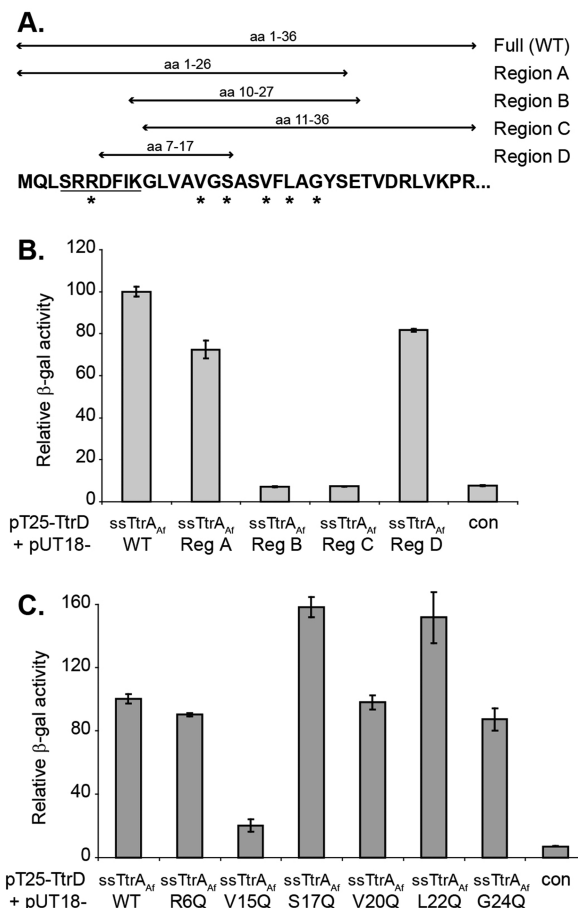


Figure 4. Analysis of the TtrD-TtrA signal peptide interaction using a bacterial two-hybrid assay. (A) Schematic figure depicting the full-length *A. fulgidus* TtrA twin-arginine signal peptide and positions of truncations (regions A–D) and glutamine substitutions (indicated by an asterisk) tested in the two-hybrid system. The twin-arginine motif is underlined. (B) The bacterial two-hybrid system of Karimova et al. was used to measure the *in vivo* interaction between TtrD and full-length TtrA signal peptide (WT) and truncated versions. (C) The bacterial two-hybrid system was used to measure the *in vivo* interaction between TtrD and variants of the TtrA signal peptide bearing single glutamine substitutions. In all assays TtrD was fused to the T25 fragment of adenylate cyclase, and the signal peptide variants were fused to T18. Output from the two-hybrid system was detected as β -galactosidase activity and expressed as a percentage of the native interaction. Bars show mean \pm SEM.

Identification of the TtrD Binding Epitope on the TtrA Signal Peptide. The BTH system was exploited in order to focus in on the minimum TtrD binding epitope within the TtrA signal peptide. The plasmid encoding the TtrA signal peptide-T18 fusion was modified to produce four truncated forms, A–D (Figure 4A). Region A comprised residues 1–26 of the TtrA signal peptide, and this showed similar binding to TtrD *in vivo* as the full length signal peptide (Figure 4B). However, constructs producing both region B (residues 10–27) and region C (residues 11–36) were essentially unable to interact with TtrD in this assay (Figure 4B). This suggested immediately that the binding epitope for TtrD on this peptide lay toward the N-terminus.

Next, site-directed mutagenesis was employed to narrow down the TtrD binding epitope still further. Glutamine residues are among the least common to be found in twin-arginine

signal peptides in general.³⁷ Here, TtrA residues R6, V15, S17, V20, L22, and G24 were substituted by glutamine (Figure 4A) and their ability to interact with TtrD assessed by BTH (Figure 4C). Of the six variants tested, only the V15Q substitution was found to interfere with TtrD binding *in vivo* (Figure 4C). Substitution of the highly conserved R6 from the targeting motif with glutamine had no impact on TtrD binding (Figure 4C). This new knowledge was then used to design a BTH construct producing only region D of the TtrA signal peptide (Figure 4A), which was observed to interact strongly with TtrD *in vivo* (Figure 4B).

Taken together, this systematic truncation and site-specific mutagenesis approach was successful in identifying TtrA signal peptide residues 7–17 as being sufficient for TtrD recognition.

Crystal Structure of *A. fulgidus* TtrD. The TtrD protein was overproduced and purified, and attempts were made to determine a structure of the complex with a TtrA signal peptide. However, crystallization experiments with either the 27-mer region A (Figure 4) or shorter 11-mer region D binding epitope identified in this work (Figure 4) were unsuccessful. The crystallization trials rather produced three new crystal forms of ligand-free TtrD distinct from that previously obtained by a structural genomics consortium (PDB entry 2idg, crystal form I). The new crystal forms provide a significant improvement in the resolution of the structure of TtrD, from 2.7 to 1.35 Å. The enhanced resolution has allowed an improvement in overall accuracy and the correction of erroneous side chain orientations found in the original deposition. The analyses also enabled an investigation regarding whether intermolecular interactions in the crystal lattice influenced the protein structure. The four crystal forms of TtrD that are now available present seven individual molecular structures. Least-squares fitting of the different structures, ~160 $\text{C}\alpha$ atoms, results in a range of RMSDs from 0.36 to 1.11 Å with an average of 0.7 Å. These data, and structural overlays (data not shown), indicate that the structures are similar irrespective of the crystalline environment in which they have been determined and it is therefore only necessary to describe a generic TtrD structure.

The TtrD molecule is a globular, single-domain protein of dimensions approximately 35 × 43 × 45 Å. There are nine α -helices, with $\alpha 1$, $\alpha 7$, $\alpha 8$, and $\alpha 9$ forming a four-helix bundle (Figure 5A). TtrD represents an archetypal thermophilic protein displaying features noted as contributing to enhanced stability (reviewed by Zhou et al.³⁸). The protein contains a pronounced hydrophobic core, formed by a number of aromatic residues (eight phenylalanines and three tyrosines), which almost surrounds the N-terminal segment of $\alpha 8$. There are 51 polar residues, 28 basic and 23 acidic, in the crystallographic model. These residues form eight salt bridge interactions plus, at numerous positions, hydrogen-bonding networks to main chain functional groups that help to hold the polypeptide in a tight globular fold with no extended loop structures.

A search of the PDB using the Dali server³⁹ identified two orthologous structures worthy of comment: the *E. coli* DmsD Tat proofreading chaperone⁴⁵ (PDB entry 3efp, Z-score 10.4, rmsd 2.7 Å for overlay of 120 $\text{C}\alpha$ positions) and the low-resolution structure of *A. fulgidus* Nar⁴⁰ (PDB entry 2o9x, Z-score 9.2, rmsd 3.1 Å for overlay of 123 $\text{C}\alpha$ positions). The overall sequence identity shared between TtrD with these two proteins is only 17 and 21%, respectively, and structural overlays primarily align the four-helix bundles (data not shown). Collectively, the three structures suggest that a small, stable,

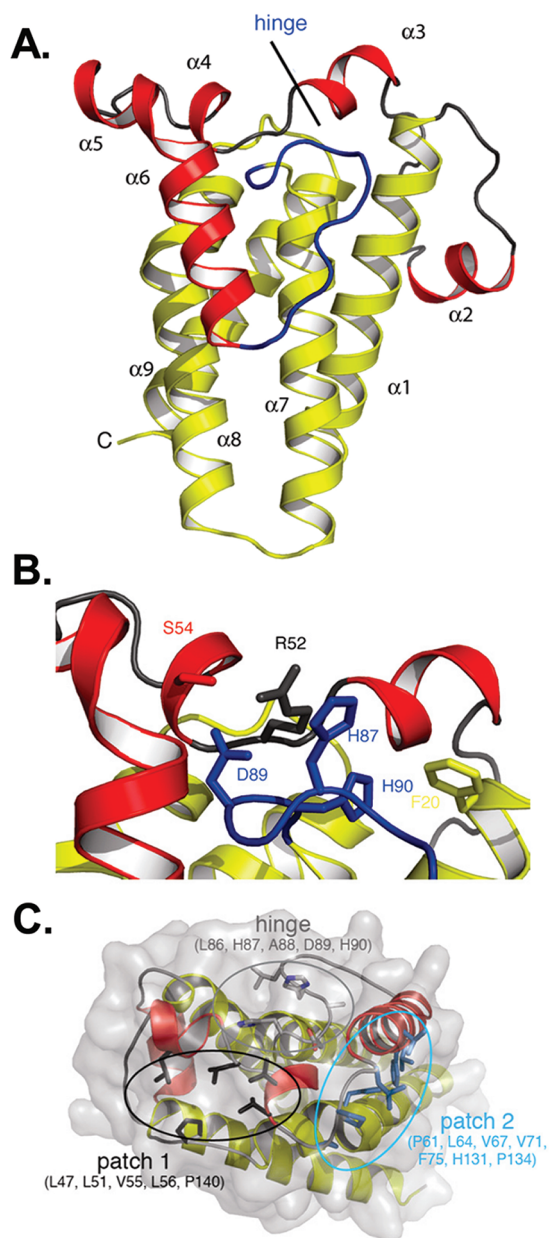


Figure 5. Crystal structure of TtrD. (A) A cartoon representation of the TtrD secondary structure. The four-helix bundle is yellow, the hinge region is blue, and peripheral helices red. (B) The functionally important His90 side-chain interacts (van der Waals) with the highly conserved Phe20. The functionally important Asp89 forms a salt bridge with Arg52 in the ligand-free structure and forms hydrogen bonds with Ser54. Arg52 may also interact with the nonconserved His87 from the hinge region. (C) The position of two hydrophobic patches on the surface of TtrD that could represent peptide binding sites. The protein is shown as a semitransparent van der Waals surface, and secondary structure is depicted as in panel A.

globular and α -helical protein fold has evolved for a peptide-binding role.

■ DISCUSSION

MGD-dependent tetrathionate reductases are an important family of respiratory enzymes, and the subcellular localization is critical to their physiological function, since the substrate is likely to be membrane impermeable. Indeed, tetrathionate is normally produced outside the prokaryotic cell by, most commonly,

an animal host during bacterial infection.¹⁹ As a result, genes for similar tetrathionate reductases can be identified in bacterial opportunistic pathogens, for example, *Salmonella*, *Proteus mirabilis*, *Bordetella parapertussis*, *Serratia marcescens*, and now also in the archaeon *A. fulgidus*. In all cases the enzymes are predicted to have similar architectures and topologies (e.g., Figure 1C) and assembly of such Tat-dependent and MGD and [Fe–S] cluster-binding enzymes would be expected to require a Tat proofreading chaperone. For example, the broadly similar heterodimeric DMSO reductase (DmsAB) from *E. coli* and *Salmonella* requires a TorD family chaperone (DmsD) for its correct assembly.^{14,41} However, subtle but interesting differences can be observed. DmsA is a member of the “type II” molybdoenzymes⁴² that contain an active-site serine or aspartate ligand to the metal. Most Type II enzymes that have been studied (NarG-type nitrate reductases, DMSO/TMAO reductases, selenate reductases) require, and are usually coexpressed with, a TorD family chaperone for correct assembly. On the other hand, tetrathionate reductase is a “type I” molybdoenzyme, which is a family of enzymes bearing cysteine or selenocysteine as active site metal ligands including the Nap-like periplasmic nitrate reductases, the respiratory formate dehydrogenases, and thiosulfate reductases.⁴² The Type I nitrate reductases require the activity of the NapD family of signal-peptide-binding proteins for assembly, which bears no relationship at all with the TorD family.⁴³ The type I formate dehydrogenases do not normally require a TorD family chaperone for assembly either, save for one example in *Campylobacter jejuni*.⁴⁴ However, in this particular case the formate dehydrogenase seems to have acquired a (type II) selenate reductase-like signal peptide and its cognate binding protein in a natural gene-shuffling event. It was a surprise, therefore, to find *ttrD* located at the 3' end of the *ttrBCA* operon in *A. fulgidus*, especially as the signal peptide itself was closely related to that of *Salmonella* TtrA, and none of the tetrathionate operons from pathogenic bacteria are clustered with a gene encoding a TorD family chaperone. Does the *Salmonella* tetrathionate reductase require a TorD family chaperone for activity? This work on the *A. fulgidus* system would imply strongly that it does, and our preliminary experiments in this area suggest that *Salmonella* DmsD, as well as the uncharacterized TorD family protein STM0610, have roles to play in tetrathionate reductase assembly in that bacterium (Guymer, D., and Sargent, F., unpublished).

In this work TtrD was found to bind directly to the TtrA signal peptide. The 11-residue TtrD binding epitope on TtrA is close to, but does not include, the conserved arginines that would be essential for protein export (Figure 4). This is an important observation because any chaperone binding motif completely reliant on these conserved arginines would immediately reduce the specificity of the peptide–chaperone interaction, and to date a general Tat chaperone that will recognize all Tat substrates in a given organism has never been identified. Indeed, despite the conservation of critical residue V15 in both *A. fulgidus* and *Salmonella* TtrA, the TtrD chaperone was unable to bind to the *Salmonella* TtrA signal peptide (data not shown), suggesting that TtrD is not a promiscuous signal-binding protein but specific for its natural partner. The location of the binding epitope near the N-terminus of the TtrA signal peptide was a surprise, however, as the *E. coli* TorD protein has been shown to bind to its cognate signal peptide at the C-terminus, well away from the conserved Tat motif.¹²

Understanding how and why TorD family proteins bind to twin-arginine signal peptides in more detail will require additional structural information. The interdomain “hinge” region noted previously in TorD family proteins,¹⁶ consensus EPxDH,⁴⁵ corresponds to the sequence stretch Leu86-His-Ala-Asp-His90 in TtrD. Unlike many other structures for TorD family proteins, this region is very well-defined in the TtrD structure. This pentapeptide forms a turn linking a region of extended structure after helix α 6 with helix α 7. These polypeptide segments form a similar structure in DmsD but are displaced relative to each other in the least-squares alignment due to a difference in the length of TtrD α 6 (data not shown). In both DmsD and TtrD the conserved aspartate (Asp89 in TtrD) makes hydrogen-bonding interactions with a conserved glycine-serine unit (Gly53-Ser54 in TtrD). The acidic side chain accepts hydrogen bonds donated from the serine amide and hydroxyl groups, and the aspartate main chain carbonyl accepts a hydrogen bond from the glycine amide. These interactions serve to connect the hinge to the α 3/ α 4 section on the surface of the protein (Figure 5B). In TtrD the Asp89 side chain also makes a hydrogen bond with the side chain of Arg52, further stabilizing this part of the protein structure. His90 is tucked down into a hydrophobic pocket near helices α 1 and α 3. The side chain donates and accepts hydrogen bonds with the Val48 carbonyl and Ala92 amide. Despite reference to this stretch of polypeptide as the “hinge”, it should be noted that TtrD cannot be correctly referred to as a “two-domain” protein. Rather, TtrD is clearly a globular, single domain, built around a central four-helix bundle.

There is no obvious, clearly defined peptide binding cleft on the surface of TtrD. It is clear that the Tat signal peptide binding epitope does not include the conserved arginine pair and instead possesses significant hydrophobic character. Therefore, an inspection of the TtrD structure was carried out to identify potential complementary features on the surface of the protein. Two hydrophobic patches are noted on either side of the conserved hinge segment. First, about 15 Å distant is a patch formed by residues on helices α 3 and α 4 and the turn linking helices α 8 and α 9. In particular, Leu47, Leu51, Val55, Leu56, and Pro140 contribute to forming a hydrophobic surface. On the other side of the hinge, closer at about 10 Å, residues from α 5 and α 7 (Pro61, Leu64, Val67, Val71, Phe75, His131, Pro134) form a potential Tat substrate-binding site (Figure 5C). This second hydrophobic patch occupies a similar position on the TtrD surface as a hydrophobic patch on the surface of DmsD, which is made from Leu82, Pro86, Trp87, and Pro124 (data not shown). Although the two protein structures are very different in this area, the conservation of a hydrophobic surface is intriguing. Indeed, DmsD Pro86 was found to be important for the signal peptide interaction, with a Pro86Gln variant having significantly impaired signal peptide binding activity.¹⁸ Moreover, a DmsD Trp87Tyr variant was found to bind the DmsA signal peptide more tightly *in vitro*, also suggesting this residue has a role to play in signal recognition.¹⁸ Further work will be required to investigate these two potential substrate-binding sites.

Concluding Remarks. Although archaea clearly utilize the Tat pathway for transport of folded proteins similar to bacteria,⁴⁶ this work now demonstrates that Tat proofreading systems are also at work in these normally extremophilic organisms. It is anticipated that the structural breakthroughs described here will lead to a greater understanding of the mechanism of signal peptide recognition on the Tat pathway.

ASSOCIATED CONTENT

S Supporting Information

Tables S1–S3. This material is available free of charge via the Internet at <http://pubs.acs.org>.

AUTHOR INFORMATION

Corresponding Author

*Tel + 44 (0)1382 386 463; Fax + 44 (0)1382 388 216; e-mail f.sargent@dundee.ac.uk.

Author Contributions

The manuscript was written through contributions of all authors.

Funding

This research was supported by the Biotechnology and Biological Sciences Research Council (Grant BB/D018986/1) and The Wellcome Trust (Grants 082596 and 083481).

Notes

The authors declare no competing financial interest.

ACKNOWLEDGMENTS

We thank Tracy Palmer (University of Dundee) for useful discussions and for providing plasmids producing AmiA, β -lactamase and GFP. We acknowledge the ESRF for synchrotron beam time and excellent staff support.

ABBREVIATIONS

DMSO, dimethyl sulfoxide; Tat, twin-arginine translocation system; TMAO, trimethylamine N-oxide; GST, glutathione S-transferase; GFP, green fluorescent protein.

REFERENCES

- (1) Sargent, F. (2007) The twin-arginine transport system: moving folded proteins across membranes. *Biochem. Soc. Trans.* **35**, 835–847.
- (2) Berks, B. C. (1996) A common export pathway for proteins binding complex redox cofactors? *Mol. Microbiol.* **22**, 393–404.
- (3) Tarry, M. J., Schafer, E., Chen, S., Buchanan, G., Greene, N. P., Lea, S. M., Palmer, T., Saibil, H. R., and Berks, B. C. (2009) Structural analysis of substrate binding by the TatBC component of the twin-arginine protein transport system. *Proc. Natl. Acad. Sci. U. S. A.* **106**, 13284–13289.
- (4) Gohlke, U., Pullan, L., McDevitt, C. A., Porcelli, I., de Leeuw, E., Palmer, T., Saibil, H. R., and Berks, B. C. (2005) The TatA component of the twin-arginine protein transport system forms channel complexes of variable diameter. *Proc. Natl. Acad. Sci. U. S. A.* **102**, 10482–10486.
- (5) Hu, Y., Zhao, E., Li, H., Xia, B., and Jin, C. (2010) Solution NMR structure of the TatA component of the twin-arginine protein transport system from gram-positive bacterium *Bacillus subtilis*. *J. Am. Chem. Soc.* **132**, 15942–15944.
- (6) Walther, T. H., Grage, S. L., Roth, N., and Ulrich, A. S. (2010) Membrane alignment of the pore-forming component TatA(d) of the twin-arginine translocase from *Bacillus subtilis* resolved by solid-state NMR spectroscopy. *J. Am. Chem. Soc.* **132**, 15945–15956.
- (7) Bageshwar, U. K., and Musser, S. M. (2007) Two electrical potential-dependent steps are required for transport by the *Escherichia coli* Tat machinery. *J. Cell Biol.* **179**, 87–99.
- (8) Lüke, I., Handford, J. I., Palmer, T., and Sargent, F. (2009) Proteolytic processing of *Escherichia coli* twin-arginine signal peptides by LepB. *Arch. Microbiol.* **191**, 919–925.
- (9) DeLisa, M. P., Tullman, D., and Georgiou, G. (2003) Folding quality control in the export of proteins by the bacterial twin-arginine translocation pathway. *Proc. Natl. Acad. Sci. U. S. A.* **100**, 6115–6120.
- (10) Sargent, F. (2007) Constructing the wonders of the bacterial world: biosynthesis of complex enzymes. *Microbiology* **153**, 633–651.

- (11) Ilbert, M., Mejean, V., and Iobbi-Nivol, C. (2004) Functional and structural analysis of members of the TorD family, a large chaperone family dedicated to molybdoproteins. *Microbiology* 150, 935–943.
- (12) Buchanan, G., Maillard, J., Nabuurs, S. B., Richardson, D. J., Palmer, T., and Sargent, F. (2008) Features of a twin-arginine signal peptide required for recognition by a Tat proofreading chaperone. *FEBS Lett.* 582, 3979–3984.
- (13) Lanciano, P., Vergnes, A., Grimaldi, S., Guigliarelli, B., and Magalon, A. (2007) Biogenesis of a respiratory complex is orchestrated by a single accessory protein. *J. Biol. Chem.* 282, 17468–17474.
- (14) Guymer, D., Maillard, J., and Sargent, F. (2009) A genetic analysis of *in vivo* selenate reduction by *Salmonella enterica* serovar Typhimurium LT2 and *Escherichia coli* K12. *Arch. Microbiol.* 191, 519–528.
- (15) Stevens, C. M., Winstone, T. M., Turner, R. J., and Paetzel, M. (2009) Structural analysis of a monomeric form of the twin-arginine leader peptide binding chaperone *Escherichia coli* DmsD. *J. Mol. Biol.* 389, 124–133.
- (16) Tranier, S., Iobbi-Nivol, C., Birck, C., Ilbert, M., Mortier-Barrière, I., Mejean, V., and Samama, J. P. (2003) A novel protein fold and extreme domain swapping in the dimeric TorD chaperone from *Shewanella massilia*. *Structure* 11, 165–174.
- (17) Jack, R. L., Buchanan, G., Dubini, A., Hatzixanthis, K., Palmer, T., and Sargent, F. (2004) Coordinating assembly and export of complex bacterial proteins. *EMBO J.* 23, 3962–3972.
- (18) Chan, C. S., Winstone, T. M., Chang, L., Stevens, C. M., Workentine, M. L., Li, H., Wei, Y., Ondrechen, M. J., Paetzel, M., and Turner, R. J. (2008) Identification of residues in DmsD for twin-arginine leader peptide binding, defined through random and bioinformatics-directed mutagenesis. *Biochemistry* 47, 2749–2759.
- (19) Winter, S. E., Thiennimitr, P., Winter, M. G., Butler, B. P., Huseby, D. L., Crawford, R. W., Russell, J. M., Bevins, C. L., Adams, L. G., Tsolis, R. M., Roth, J. R., and Baumler, A. J. (2010) Gut inflammation provides a respiratory electron acceptor for *Salmonella*. *Nature* 467, 426–429.
- (20) Karimova, G., Pidoux, J., Ullmann, A., and Ladant, D. (1998) A bacterial two-hybrid system based on a reconstituted signal transduction pathway. *Proc. Natl. Acad. Sci. U. S. A.* 95, 5752–5756.
- (21) Karimova, G., Ullmann, A., and Ladant, D. (2001) Protein-protein interaction between *Bacillus stearothermophilus* tyrosyl-tRNA synthetase subdomains revealed by a bacterial two-hybrid system. *J. Mol. Microbiol. Biotechnol.* 3, 73–82.
- (22) Tabor, S., and Richardson, C. C. (1985) A bacteriophage T7 RNA polymerase/promoter system for controlled exclusive expression of specific genes. *Proc. Natl. Acad. Sci. U. S. A.* 82, 1074–1078.
- (23) Miller, J. H. (1972) *Experiments in Molecular Genetics*, Cold Spring Harbor Laboratory, Cold Spring Harbor, NY.
- (24) Kabsch, W. (1993) Automatic Processing of Rotation Diffraction Data from Crystals of Initially Unknown Symmetry and Cell Constants. *J. Appl. Crystallogr.* 26, 795–800.
- (25) Leslie, A. G. (2006) The integration of macromolecular diffraction data. *Acta Crystallogr., Sect. D: Biol. Crystallogr.* 62, 48–57.
- (26) Evans, P. (2006) Scaling and assessment of data quality. *Acta Crystallogr., Sect. D: Biol. Crystallogr.* 62, 72–82.
- (27) McCoy, A. J., Grosse-Kunstleve, R. W., Adams, P. D., Winn, M. D., Storoni, L. C., and Read, R. J. (2007) Phaser crystallographic software. *J. Appl. Crystallogr.* 40, 658–674.
- (28) Emsley, P., and Cowtan, K. (2004) Coot: model-building tools for molecular graphics. *Acta Crystallogr., Sect. D: Biol. Crystallogr.* 60, 2126–2132.
- (29) Murshudov, G. N., Vagin, A. A., and Dodson, E. J. (1997) Refinement of macromolecular structures by the maximum-likelihood method. *Acta Crystallogr., Sect. D: Biol. Crystallogr.* 53, 240–255.
- (30) Painter, J., and Merritt, E. A. (2006) TLSMD web server for the generation of multi-group TLS models. *J. Appl. Crystallogr.* 39, 109–111.
- (31) Hensel, M., Hinsley, A. P., Nikolaus, T., Sawers, G., and Berks, B. C. (1999) The genetic basis of tetrathionate respiration in *Salmonella typhimurium*. *Mol. Microbiol.* 32, 275–287.
- (32) Ize, B., Stanley, N. R., Buchanan, G., and Palmer, T. (2003) Role of the *Escherichia coli* Tat pathway in outer membrane integrity. *Mol. Microbiol.* 48, 1183–1193.
- (33) Stanley, N. R., Sargent, F., Buchanan, G., Shi, J., Stewart, V., Palmer, T., and Berks, B. C. (2002) Behaviour of topological marker proteins targeted to the Tat protein transport pathway. *Mol. Microbiol.* 43, 1005–1021.
- (34) Ize, B., Coulthurst, S. J., Hatzixanthis, K., Caldelari, I., Buchanan, G., Barclay, E. C., Richardson, D. J., Palmer, T., and Sargent, F. (2009) Remnant signal peptides on non-exported enzymes: implications for the evolution of prokaryotic respiratory chains. *Microbiology* 155, 3992–4004.
- (35) Li, S. Y., Chang, B. Y., and Lin, S. C. (2006) Coexpression of TorD enhances the transport of GFP via the TAT pathway. *J. Biotechnol.* 122, 412–421.
- (36) DeLisa, M. P., Samuelson, P., Palmer, T., and Georgiou, G. (2002) Genetic analysis of the twin arginine translocator secretion pathway in bacteria. *J. Biol. Chem.* 277, 29825–29831.
- (37) Cristóbal, S., de Gier, J. W., Nielsen, H., and von Heijne, G. (1999) Competition between Sec- and TAT-dependent protein translocation in *Escherichia coli*. *EMBO J.* 18, 2982–2990.
- (38) Zhou, X. X., Wang, Y. B., Pan, Y. J., and Li, W. F. (2008) Differences in amino acids composition and coupling patterns between mesophilic and thermophilic proteins. *Amino Acids* 34, 25–33.
- (39) Holm, L., and Rosenstrom, P. (2010) Dali server: conservation mapping in 3D. *Nucleic Acids Res.* 38, W545–549.
- (40) Kirillova, O., Chruszcz, M., Shumilin, I. A., Skarina, T., Gorodichtchenskaia, E., Cymborowski, M., Savchenko, A., Edwards, A., and Minor, W. (2007) An extremely SAD case: structure of a putative redox-enzyme maturation protein from *Archaeoglobus fulgidus* at 3.4 Å resolution. *Acta Crystallogr., Sect. D: Biol. Crystallogr.* 63, 348–354.
- (41) Oresnik, I. J., Ladner, C. L., and Turner, R. J. (2001) Identification of a twin-arginine leader-binding protein. *Mol. Microbiol.* 40, 323–331.
- (42) Kisker, C., Schindelin, H., and Rees, D. C. (1997) Molybdenum-cofactor-containing enzymes: structure and mechanism. *Annu. Rev. Biochem.* 66, 233–267.
- (43) Maillard, J., Spronk, C. A., Buchanan, G., Lyall, V., Richardson, D. J., Palmer, T., Vuister, G. W., and Sargent, F. (2007) Structural diversity in twin-arginine signal peptide-binding proteins. *Proc. Natl. Acad. Sci. U. S. A.* 104, 15641–15646.
- (44) Hitchcock, A., Hall, S. J., Myers, J. D., Mulholland, F., Jones, M. A., and Kelly, D. J. (2010) Roles of the twin-arginine translocase and associated chaperones in the biogenesis of the electron transport chains of the human pathogen *Campylobacter jejuni*. *Microbiology* 156, 2994–3010.
- (45) Turner, R. J., Papish, A. L., and Sargent, F. (2004) Sequence analysis of bacterial redox enzyme maturation proteins (REMPs). *Can. J. Microbiol.* 50, 225–238.
- (46) Rose, R. W., Brüser, T., Kissinger, J. C., and Pohlschroder, M. (2002) Adaptation of protein secretion to extremely high-salt conditions by extensive use of the twin-arginine translocation pathway. *Mol. Microbiol.* 45, 943–950.